

DESY 85-090  
August 1985



ELECTROWEAK INTERFERENCE EFFECTS IN  $e^+e^-$  INTERACTIONS  
AND SELECTED RESULTS ON  $\tau$  DECAYS

by

B. Naroska

*Deutsches Elektronen-Synchrotron DESY, Hamburg*

ISSN 0418-9833

NOTKESTRASSE 85 · 2 HAMBURG 52

**DESY behält sich alle Rechte für den Fall der Schutzrechtserteilung und für die wirtschaftliche Verwertung der in diesem Bericht enthaltenen Informationen vor.**

**DESY reserves all rights for commercial use of information included in this report, especially in case of filing application for or grant of patents.**

**To be sure that your preprints are promptly included in the  
HIGH ENERGY PHYSICS INDEX ,  
send them to the following address ( if possible by air mail ) :**

**DESY  
Bibliothek  
Notkestrasse 85  
2 Hamburg 52  
Germany**

**ELECTROWEAK INTERFERENCE EFFECTS IN  $e^+e^-$  INTERACTIONS  
AND SELECTED RESULTS ON  $\tau$  DECAYS**

BEATE NAROSKA  
DESY  
NOTKESTR. 85  
D 2000 HAMBURG 52

**1. INTRODUCTION**

The first part of this review will give recent results on electroweak interference effects in  $e^+e^-$  interactions. Data from  $e^+e^- \rightarrow e^+e^-$ ,  $\mu^+\mu^-$ ,  $\tau^+\tau^-$  and  $e^+e^- \rightarrow$  hadrons are now available over a large range of center of mass (cm) energies,  $12 \leq \sqrt{s} \leq 46.8$  GeV. From the lepton pair production data weak coupling parameters will be deduced and compared with measurements in neutrino interactions, at the  $p\bar{p}$  collider and with predictions of the standard model<sup>1)</sup>. The total cross-section for the production of hadrons will be compared to electroweak and QCD predictions. Measurements of the charge asymmetry for c and b quarks will be used to calculate their axial couplings.

In the second part, recent results on  $\tau$  decays will be reviewed, namely the measurements of topological branching ratios, leptonic branching ratios and new limits on the mass of the  $\nu_\tau$ .

**2. ELECTROWEAK CROSS-SECTIONS**

The differential cross-section for  $e^+e^- \rightarrow f^+f^-$ , where f can be  $\mu, \tau$  or a quark of charge  $Q_f$ , taking into account interference between the photon and  $Z^0$  exchange is in lowest order given by<sup>2)</sup>:

$$\frac{d\sigma}{d\Omega} = \frac{\alpha^2}{4s} \cdot (C_1 \cdot (1 + \cos^2 \theta) + C_2 \cdot \cos \theta) \quad (1)$$

where

$$C_1 = Q_f^2 \cdot 2 \cdot Q_f \cdot v_e v_f \chi + (v_e^2 + a_e^2) \cdot (v_f^2 + a_f^2) \cdot \chi^2$$

$$C_2 = -4 \cdot Q_f \cdot a_e a_f \chi + 8 v_e v_f a_e a_f \cdot \chi^2$$

$v_e, v_f, a_e$  and  $a_f$  denote the vector and axial-vector weak couplings of electron and fermion f. In the standard model  $a_f$  is given by the third component of the weak isospin  $T_3$ ,  $a_f = 2(T_{3L} - T_{3R})$ , and  $v_f = 2(T_{3L} + T_{3R}) - 4 \cdot Q_f \cdot \sin^2 \theta_W$ , where  $\sin^2 \theta_W$  is the mixing angle, which describes the relative strength of weak neutral to electromagnetic current. With the weak isospin assignments of the standard model,  $T_{3L} = -\frac{1}{2}$  and  $T_{3R} = 0$  the, the weak coupling constants of the leptons are  $a_f = -1$  and  $v_f = -0.12$  with  $\sin^2 \theta_W = 0.22$ .

The forward-backward asymmetry is defined as  $\frac{N_F - N_B}{N_F + N_B}$ , where  $N_F$  and  $N_B$  are the numbers of events in the forward and backward hemisphere<sup>1)</sup>; it is given by:

$$A = \frac{3}{8} \cdot \frac{C_2}{C_1} \sim -1.5 \cdot \frac{a_e a_f}{Q_f} \chi \quad (2)$$

The approximation is due to neglecting terms with  $\chi^2$ , which is still good to a one percent accuracy even at the highest PETRA energy. The asymmetry is thus mainly sensitive to the axial weak coupling.

The total cross-section ratio:

$$R = \frac{\sigma_{had}}{\sigma_{O(\alpha^2)}} = C_1 \quad \text{with} \quad \sigma_{O(\alpha^2)} = \frac{4\pi\alpha^2}{3s} \quad (3)$$

will be used to obtain limits on the vector coupling constants.

Two parametrizations are currently used for  $\chi$ :

$$\chi_I = \frac{G_F M_Z^2}{8\pi\alpha\sqrt{2}} \frac{s}{s - M_Z^2} \quad \text{and} \quad \chi_{II} = \frac{1}{16\sin^2 \theta_W} \frac{s}{\cos^2 \theta_W s - M_Z^2}$$

In parametrization I the free parameters in  $e^+e^-$  are  $M_Z, \alpha$  and the Fermi constant  $G_F$ ;  $\alpha$  and  $G_F$  have been determined accurately<sup>7)</sup>. In parametrization II  $\alpha, \sin^2 \theta_W$  and  $M_Z$  are free parameters.

<sup>1)</sup> Forward is defined by the particle  $f^-$  being scattered with an angle  $\theta < 90^\circ$  with respect to the  $e^-$ -beam.

**ABSTRACT**

Results on  $e^+e^- \rightarrow \mu^+\mu^-$  and  $\tau^+\tau^-$  from PEP and PETRA are reviewed. The forward-backward asymmetry predicted by electroweak interference is established up to  $s \sim 2000$  GeV<sup>2</sup>. Weak axial-vector and vector coupling constants are determined and agree with the predictions of the standard model within 1-2 standard deviations.  $\mu - \tau$  universality is confirmed within statistics but a small difference is not excluded at high energies. The muon data exclude an infinite Z-mass with more than 99% confidence level. For  $e^+e^- \rightarrow$  hadrons the total cross-section shows the rise predicted by electroweak interference. The angular asymmetries of c and b quark have been measured by several experiments leading to world averages of the c and b axial coupling constants which agree with the standard model prediction assuming the usual fractional charges.

Numerous new results are available on  $\tau$  decays: topological branching ratios into 1, 3 and also 5 charged particles have been measured as well as the leptonic branching ratios. Improved measurements have reduced the upper limit of the mass of the  $\nu_\tau$  to  $\sim 70$  MeV.

Invited talk given at "Physics in Collisions V", July 1985, Autun, France. Part of the material was also used for a talk at the "Workshop on Tests of Electroweak Theories", June 1985, Trieste, Italy

Table 1. Asymmetries for  $e^+e^- \rightarrow \mu^+\mu^-$

Experiment	$\sqrt{s}$ (GeV)	$\int Ldt$ (pb $^{-1}$ )	Events	$A_{\mu\mu}$ (%)	$A_{SLM}$ (%)	Ref
HRS	29	106	5057	$-4.9 \pm 1.5 \pm 0.5$	-5.9	21
MAC	29	226.2	16058	$-5.75 \pm 0.85 \pm 0.2$	-5.9	22
MARK II	29	100	5312	$-7.1 \pm 1.7$	-5.9	23
AV. PEP	29	432	26427	$-5.81 \pm 0.69$	-5.9	
CELLO	34.2	11.3	387	$-6.4 \pm 6.4$	-8.6	10
JADE	34.4	71.2	3400	$-11.0 \pm 1.8 \pm 1.0$	-8.7	12
MARK J	34.6	76.3	3658	$-11.7 \pm 1.7 \pm 0.5$	-8.8	14,16
PLUTO	34.7	44.0	1550	$-12.4 \pm 3.1 \pm 1.0$	-8.9	17,18
TASSO	34.5	74.7	2673	$-9.1 \pm 2.3 \pm 0.5$	-8.8	19
AV. PETRA	34.5	277.5	11668	$-10.9 \pm 1.1$	-8.8	
CELLO	43.9	21.0	430	$-17.2 \pm 5.9$	-15.7	11
JADE	43.1	26.4	833	$-19.5 \pm 3.5$	-15.0	13
MARK J	43.1	32.8	1014	$-15.5 \pm 3.4$	-15.0	16
TASSO	43.7	25.1	450	$-19.0 \pm 5.0$	-15.4	20
AV. PETRA	43.4	105.3	2727	$-17.9 \pm 2.0$	-15.4	

Table 2. Asymmetries for  $e^+e^- \rightarrow r^+r^-$

Experiment	$\sqrt{s}$ (GeV)	$\int Ldt$ (pb $^{-1}$ )	Events	$A_{rr}$ (%)	$A_{SLM}$ (%)	Ref
HRS	29	185	5301	$-5.2 \pm 1.7 \pm 0.5$	-5.9	31
MAC	29	210	10153	$-5.5 \pm 1.2 \pm 0.5$	-5.9	32
MARK II	29	100	3714	$-4.2 \pm 2.0$	-5.9	23
AV. PEP	29	416	19168	$-5.1 \pm 0.9$	-5.9	
CELLO	34.2	17.0	434	$-10.3 \pm 5.2$	-8.6	26
JADE	34.6	62.4	1998	$6.0 \pm 2.5 \pm 1.0$	-8.8	27
MARK J	34.6	79.6	758	$-8.5 \pm 4.8$	-8.8	15
PLUTO	34.6	42.3	419	$-5.9 \pm 6.8 \pm 2.5$	-8.8	29
TASSO	34.5	69.4		$-4.9 \pm 5.3 \pm 1.2$	-8.8	30
AV. PETRA	34.6	270.7	3579	$-6.8 \pm 1.9$	-8.8	
CELLO	43.9	21.0	397	$-14.2 \pm 4.8 \pm 1.0$	-15.7	11
JADE	43.1	26.6	575	$-11.8 \pm 4.6 \pm 1.0$	-14.9	27
MARK J	43.1	32.8	272	$-13.0 \pm 6.4$	-15.3	28
AV. PETRA	43.3	80.4	1244	$-13.0 \pm 3.0$	-15.4	

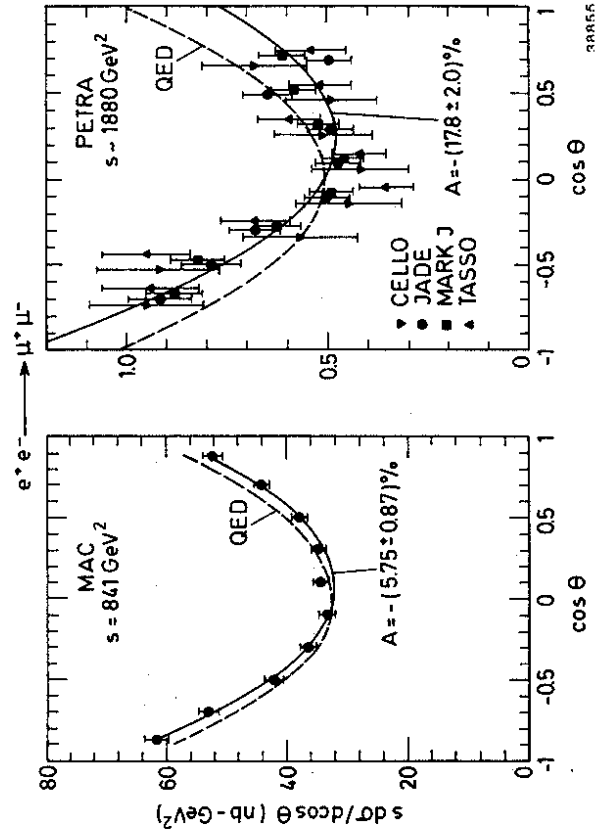


Figure 1 Angular distributions for  $e^+e^- \rightarrow \mu^+\mu^-$  a) from MAC at  $\sqrt{s}=29$  GeV b) from the 4 PETRA experiments at  $\langle \sqrt{s} \rangle = 43.4$  GeV.

In lowest order the two definitions of  $\chi$  are the same, they can be transformed into each other using the relation  $M_Z^2 = \pi\alpha/(\sqrt{2}G_F \sin^2\theta_W \cos^2\theta_W)$ . If electroweak one-loop corrections are taken into account, a small correction has to be applied to the asymmetry when using  $\chi^{(3)}$ . For parametrization II the one-loop corrections cancel fortuitously<sup>4,5,6)</sup>. Taking into account the one-loop corrections the predictions for the asymmetry are the same in both parametrizations with the input values  $\sin^2\theta_W = 0.217$ ,  $M_Z = 93$  GeV and  $\alpha$  and  $G_F$  as in <sup>7)</sup>. Therefore also the result for the weak coupling constants is unambiguous; there is, however, a difference in the error of the prediction due to the uncertainty of the Z-mass: it is larger in parametrization II (see fig. 8). Parametrization II, on the other hand, allows to place tighter constraints on  $\sin^2\theta_W$  or  $M_Z$  in  $e^+e^-$  collisions if the assignment of  $a$  and  $v$  of the standard model are used.

### 3. LEPTONIC REACTIONS

#### 3.1 $e^+e^- \rightarrow \mu^+\mu^-$

The differential and total cross-sections for muon pairs have been measured by almost all groups working on the two storage rings PEP and PETRA; the CELLO, JADE, MARK J, PLUTO and TASSO collaborations work at PETRA; the HRS, MAC and MARK II collaborations work at PEP. PEP has run at  $\sqrt{s}=29$  GeV only and some experiments have accumulated more than 200 pb $^{-1}$ , though not all the data have been analysed in all experiments. MAC has the highest statistics in muon pairs, they have analysed more than 16000 muon pairs, corresponding to 226 pb $^{-1}$  (fig. 1a). PETRA on the other hand has followed a program to increase the center of mass energy. The highest energy of  $\sqrt{s}=46.78$  GeV was reached in spring of 1984. Since then the energy has been reduced to obtain higher luminosities. This review includes PETRA data up to the end of 1984 the analysis of which is almost final (fig 1b).

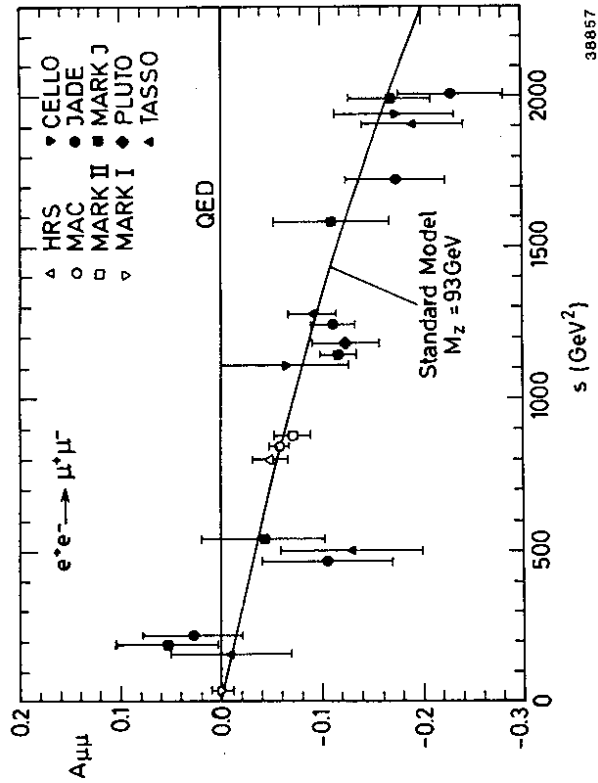


Figure 2 The angular asymmetry for  $e^+e^- \rightarrow \mu^+\mu^-$  as a function of  $s$ . The data are corrected for  $\alpha^3$  QED effects. The solid line is the prediction of the standard model using  $X_{II}$  with  $\sin^2 \theta_W = 0.217$  and  $M_Z = 93$  GeV.

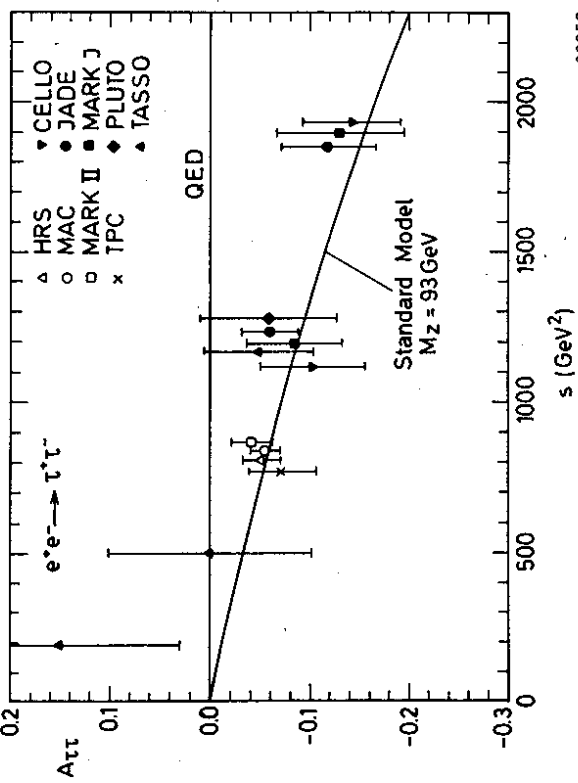


Figure 3 The angular asymmetry for  $e^+e^- \rightarrow \tau^+\tau^-$  as a function of  $s$ . The data are corrected for  $\alpha^3$  QED effects. The solid line is the prediction of the standard model using  $X_{II}$  with  $\sin^2 \theta_W = 0.217$  and  $M_Z = 93$  GeV.

The data samples for muon pairs typically have an angular acceptance of  $|\cos\theta| \leq 0.8$  where  $\theta$  is the scattering angle of the muon with respect to the beam axis. The muons are demanded to be collinear within  $10^\circ$  to reduce the number of  $\mu\mu\gamma$  events. The background from other processes, like  $e\mu\mu$ ,  $\tau^+\tau^-$  and cosmic rays, is usually below a few percent.

The data presented in table 1 and figs. 1-4 are corrected for  $\alpha^3$  effects from QED.<sup>1</sup> The QED corrections were computed using programs by Berends et al.<sup>5,26</sup> and they are detector dependent. The corrections for the total event rates are small but they have a forward-backward asymmetry of about +2%. The asymmetry values in tables 1 and 2 and figures 2 and 3 are extrapolated to  $|\cos\theta| = 1$  in order to make them independent of the experimental acceptance cuts.

The "electroweak" one-loop corrections which depend on the parameterization of  $\chi$  (see chapter 2) were incorporated in the theoretical value of the standard model  $As_{M.M.}$  with which the data are compared<sup>8</sup>. The measured asymmetries are listed in table 1 and have been averaged at three cm energies: 29, 34.5 and 43.4 GeV. The average values agree with the predictions of the standard model within 1, 2 and 1 standard deviations at these three energies; each is  $\sim 10$  standard deviations away from 0. If weak interactions would proceed without an intermediate boson ( $M_Z \rightarrow \infty$  in  $X_I$ ) smaller asymmetries would be predicted, which are 2.5 standard deviations below the measured value at the two PETRA energies. The asymmetries are shown as a function of  $s$  in fig. 2.

In fig. 4 the measured R values are shown. They agree well with QED and the standard model which is indistinguishable from QED even at the highest energies.

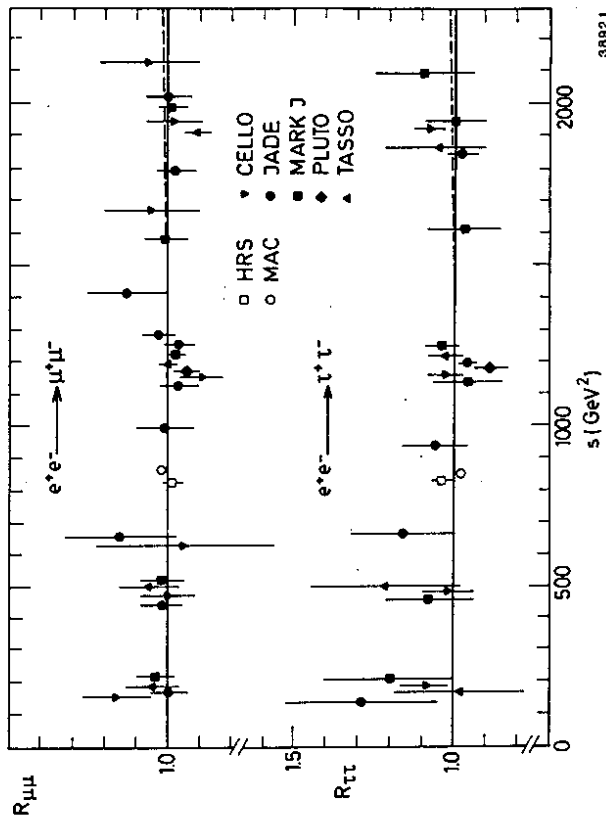


Figure 4 Total Cross-Section Ratios as functions of  $s$  for  $e^+e^- \rightarrow \mu^+\mu^-$  and  $e^+e^- \rightarrow \tau^+\tau^-$ . The QED (full line) and standard model predictions (broken line) are also shown. The errors are statistical only. Estimates of the normalisation error range between 3 and 5%.

<sup>1</sup>If an additional electroweak correction was applied to the asymmetry by the authors, it was removed in order to make the data comparable.

### 3.2 $e^+e^- \rightarrow \tau^+\tau^-$

The  $\tau$  decays before it enters the detector, so it has to be recognized through its decay products, which are mainly leptons and charged and neutral pions. Efficient  $\tau$  analysis therefore requires the possibility of identifying electrons, muons and photons in a large solid angle. Furthermore certain topologies are usually not selected due to overwhelming background, e.g. both  $\tau$ 's decaying into a muon or both into an electron or both into more than 3 charged particles. The " $\tau$  efficiencies" achieved by the experiments, i.e. the ratio of the number of events used in the asymmetry analysis to the number of events expected from the lowest order cross-section, range between 20-50%.

The asymmetry data corrected for pure QED like the muon pairs (see chapter 3.1) are listed in table 2. The angular distribution obtained by the CELLO Collaboration at  $\sqrt{s} \sim 43.6 \text{ GeV}^{(1)}$  is shown as an example in fig. 5. The asymmetries are shown as a function of  $s$  in fig. 3, the R-values in fig. 4.

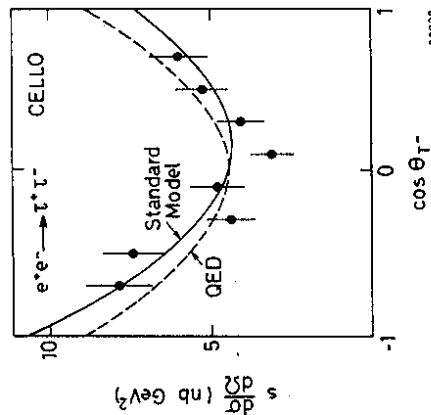


Figure 5 Angular distribution for  $e^+e^- \rightarrow \tau^+\tau^-$  from CELLO

### 3.3 Determination of Coupling Constants.

The vector coupling constants were determined for each experiment using their measured cross-section ratios and eq. (3) with  $\chi_I$  and  $M_Z = 93 \text{ GeV}$  and assuming  $a_e a_f = 1$ . The results which are shown in fig. 6, are close to 0 everywhere. This reflects the good agreement of the measured values with the electroweak or QED predictions.

The axial-vector coupling constants were calculated for each experiment from the measured asymmetries using eq. (2) with  $\chi_I$  and assuming  $|a_e| = 1$ . They are shown in fig. 7 for muons and taus. They agree within errors with each other and with the standard model prediction. In fig. 8 they are averaged in the same three energy bins as in tables 1 and 2. The values are:

$\sqrt{s}(\text{GeV})$	$ a_\mu $	$ a_\tau $
PEP 29	$0.99 \pm 0.12$	$0.88 \pm 0.16$
PETRA 34.5	$1.27 \pm 0.13$	$0.79 \pm 0.22$
PETRA 43.4	$1.16 \pm 0.13$	$0.85 \pm 0.20$
ALL	$1.13 \pm 0.07$	$0.85 \pm 0.11$

As noticed before<sup>(9)</sup>, at  $s \sim 1200 \text{ GeV}^2$   $a_\mu$  is two standard deviations higher than the prediction. At the highest Petra energy of  $\sim 1850 \text{ GeV}^2$   $a_\mu$  still comes out high but the difference to the prediction is only one standard deviation.

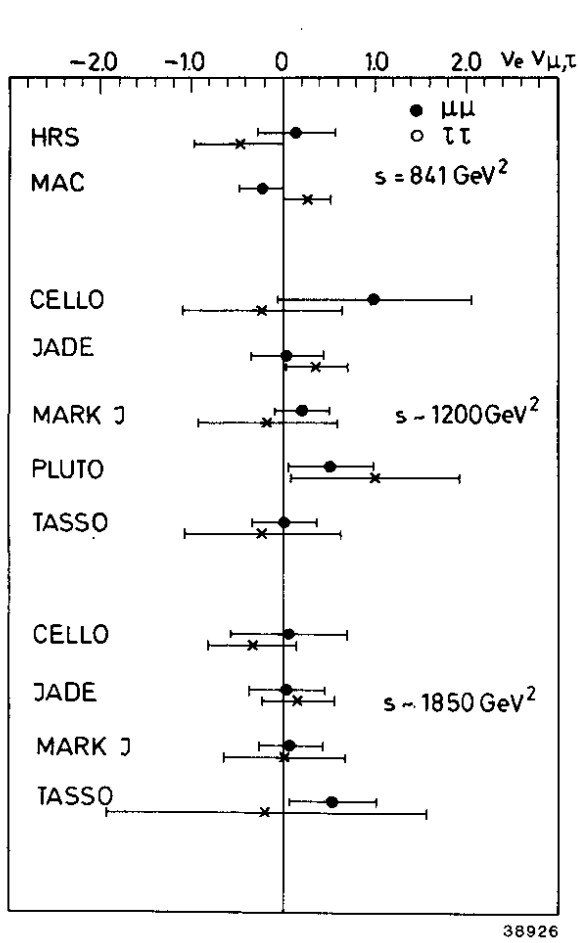


Figure 6 Vector coupling constants calculated from measured cross-sections for muons and taus.  $M_Z = 93 \text{ GeV}$  and  $\sin^2 \theta_W = 0.217$  were used and  $a_e a_f = 1$  was assumed.

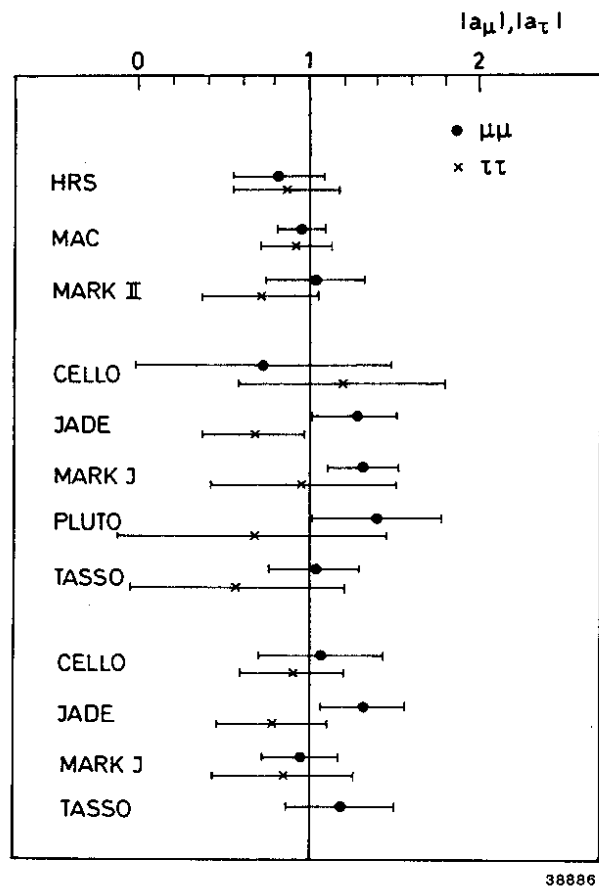


Figure 7 Axial-vector coupling constants calculated from measured asymmetries for muons and taus.  $M_Z = 93 \text{ GeV}$  and  $\sin^2 \theta_W = 0.217$  were used,  $a_e = 1$  was assumed.

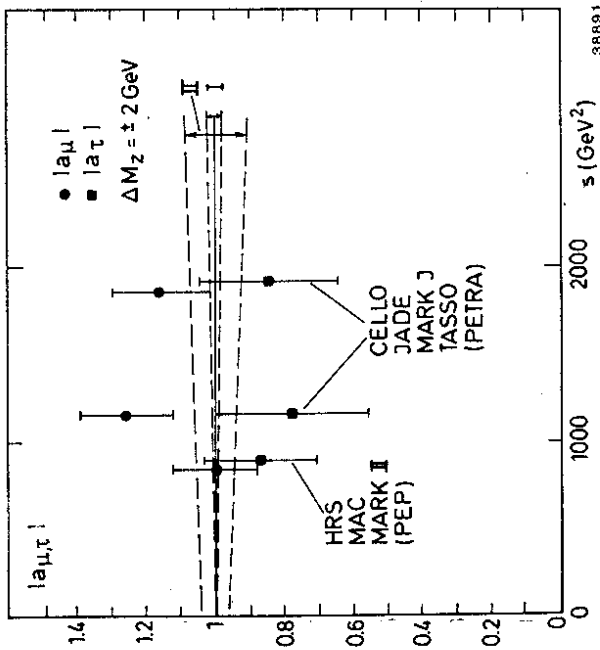


Figure 8 Average axial-vector coupling constants at three values of  $s$  for muons and taus.  $M_Z = 93$  GeV and  $\sin^2 \theta_W = 0.217$  were used. The broken lines indicate the uncertainty due to  $\Delta M_Z = \pm 2$  GeV for the two different parametrizations of  $\chi$ .

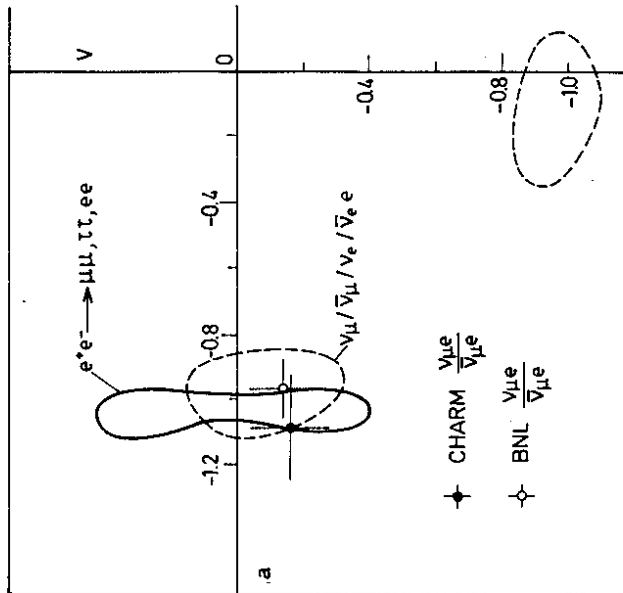


Figure 9 95% confidence level contours in the  $(a, v)$  plane.  $e^+e^-$  results (full line) are compared to averaged  $\nu_e$  results (dashed lines).

The axial-vector coupling constants of the taus at high energy have in contrast to muon pairs a tendency to lie somewhat lower than the predicted value. The average differences  $(a_\mu) - (a_\tau)$  are  $0.12 \pm 0.20$ ,  $0.47 \pm 0.25$  and  $0.31 \pm 0.24$  at the average  $s$ -values of 841, 1200 and 1850  $\text{GeV}^2$ , respectively. Within errors  $\mu$ - $\tau$  universality is confirmed, but a small difference cannot be excluded (fig. 8). Assuming  $e$ - $\mu$ - $\tau$  universality the vector and axial-vector coupling constants were determined in two parameter fits. The measured asymmetries and  $R$ -values for  $e^+e^- \rightarrow \mu^+\mu^-$  and  $\tau^+\tau^-$  were used as input data. In addition Bhabha data were used from MAC<sup>34)</sup> at  $\sqrt{s} = 29$  GeV, JADE<sup>35)</sup>, PLUTO<sup>18)</sup> and TASSO<sup>19,36)</sup> at  $\sqrt{s} \sim 34.5$  GeV and 43.5 GeV. The resulting values (world average) are:

$$\left. \begin{array}{l} |a| = 1.03 \pm 0.04 \\ |v| = 0.29 \pm 0.10 \end{array} \right\} \text{for } e, \mu, \tau \text{ combined}$$

in good agreement with the predictions of the standard model. The effect of the Bhabha data is a reduction of the error of the vector coupling constant.

In fig. 9 the 95% confidence level contours of this fit (the symmetric solution at  $-|v|$  is not shown) in the  $(a, v)$ -plane are compared to the contours from neutrino scattering on electrons<sup>37)</sup>, which were calculated from the measured cross-sections. Good agreement of  $e^+e^-$  data and neutrino data is observed. The crosses in fig. 9 were obtained from the measured ratio of  $\sigma(\nu_\mu e) / \sigma(\bar{\nu}_\mu e)$ , which yields a measurement of the coupling constants at low  $Q^2$  almost free from systematic errors<sup>38)</sup>. They are however not independent of the neutrino contours (again the three symmetric solutions in the other three quadrants are not shown).

### 3.4 Determination of $\sin^2 \theta_W$ or $M_Z$ .

An alternative way of comparing the data with electroweak predictions is by determining constraints on the electroweak mixing angle  $\sin^2 \theta_W$  and the mass of the  $Z^0$  boson. The weak isospin structure of the standard model is assumed and the values of  $a$  and  $v$  are therefore predicted. Using parametrization II of  $\chi$  with  $M_Z = (93 \pm 2)$  GeV as measured at the  $p\bar{p}$  collider<sup>40)</sup> one determines from the combined data from muons and taus:

$$\sin^2 \theta_W = 0.21 \pm 0.019 \pm 0.013$$

The second error is due to the uncertainty in the  $Z$ -mass. For comparison,  $\sin^2 \theta_W = 0.217 \pm 0.014$  is the radiatively corrected<sup>41)</sup> world average value, which comes mainly from deep inelastic  $\nu_\mu$  scattering. The average value from neutrino scattering on electrons which includes recent results not contained in the above average is  $\sin^2 \theta_W = 0.211 \pm 0.028$ <sup>38)</sup>.

The result for  $\sin^2 \theta_W$  from  $e^+e^- \rightarrow \mu^+\mu^-$  alone is  $0.18 \pm 0.02$ , about two standard deviations below the neutrino data, while the taus give  $\sin^2 \theta_W = 0.27 \pm 0.06$ , one standard deviation higher.

Alternatively one can use as input  $\sin^2 \theta_W = 0.217 \pm 0.014$  from neutrino scattering and determines from muon pairs and taupair data:  $M_Z = (91.7 \pm 1) \text{ GeV}$  in good agreement with the  $p\bar{p}$  collider data.

### 4. $e^+e^- \rightarrow \text{HADRONS}$

At present two methods are used to compare electroweak predictions for quarks with the data. The separation of quark flavours and the determination of a charge asymmetry has been successful only for  $c$ - and  $b$ -quarks. An attempt to test the predictions also for light quarks has been made by analyzing the total cross-section data. The electroweak effects in the total hadronic cross-sections are predicted to be larger than for leptons due to the larger vector coupling constants of the quarks,  $v_f = 0.41$  for  $f = u, c$  and  $v_f = -0.71$  for  $f = d, s, b$ . But as all quarks are mixed in the hadronic final states, only global statements are possible.

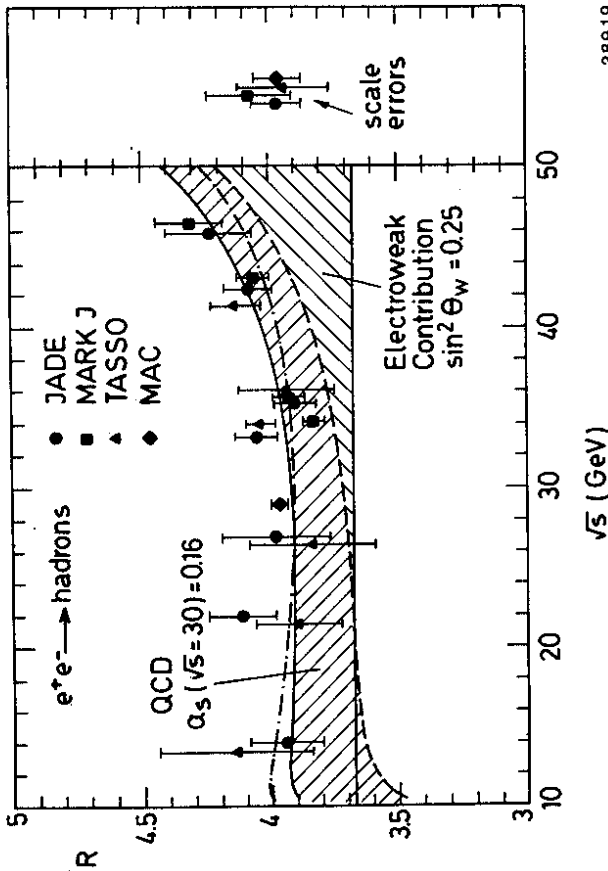


Figure 10 Total cross-section measurements  $e^+e^- \rightarrow \text{hadrons}$  as a function of  $\sqrt{s}$ . For details see text.

#### 4.1 Total Cross-Section.

The total cross-section for  $e^+e^- \rightarrow \text{hadrons}$  is in the quark-parton-model with mass-less partons:

$$R_{\text{had}} = \frac{\sigma_{\text{had}}}{\sigma_{\mu\mu}} = 3 \cdot \sum_f Q_f^2$$

The sum runs over the flavours  $f$ ,  $f=u,d,s,c$  and  $b$  at presently available energies. For massive quarks with velocity  $\beta$  the electroweak cross-section with QCD corrections is in lowest order<sup>42)</sup>:

$$R_{\text{had}} = 3 \cdot \sum_f \frac{1}{2} (3\beta - \beta^3) \cdot C_{VV} + \beta^3 \cdot C_{AA} + \left(\frac{\alpha_s}{\pi}\right) \cdot [r_{\text{tot}} \cdot C_{VV} + r'_{\text{tot}} C_{AA}] \quad (4)$$

where

$$C_{VV} = Q_f^2 - 2Q_f v_z v_f \chi + (v_z^2 + a_z^2) v_f^2 \chi^2$$

$$C_{AA} = (v_z^2 + a_z^2) a_f^2 \chi^2$$

The QCD correction functions  $r_{\text{tot}}$  and  $r'_{\text{tot}}$  the so called Schwinger terms, depend only on  $2m_f/\sqrt{s}$  ( $m_f$  is the quark mass); for  $m_f/\sqrt{s} \rightarrow 0$  the QCD correction reduces to the well known  $1 + \alpha_s/\pi$ .

The three PETRA experiments JADE<sup>43)</sup>, MARK J<sup>44)</sup> and TASSO<sup>45)</sup> have analyzed the total cross-section of  $e^+e^- \rightarrow \text{hadrons}$  up to the highest PETRA energies. Their data are shown in fig. 10 together with the value from MAC<sup>46)</sup> at  $\sqrt{s} = 29$  GeV. The point-to-point systematic errors are included in the error bars. The total normalization errors of 2.5%, 4.0%, 4.5% and 2.3% respectively are shown separately.

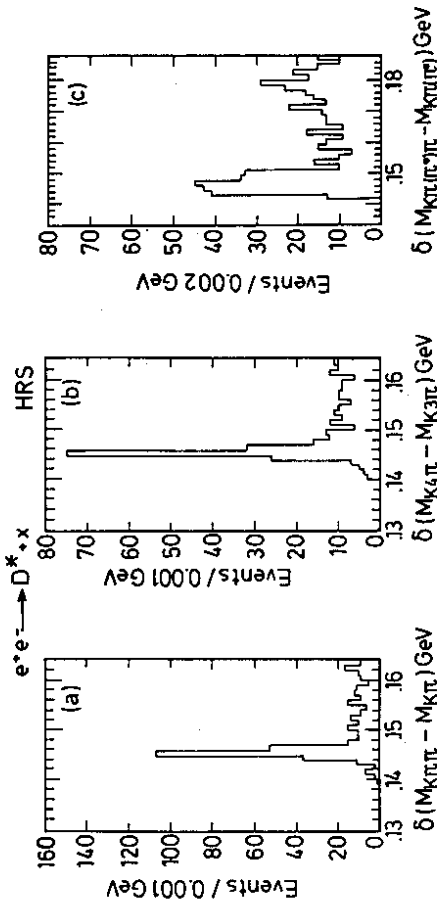


Figure 11  $\delta$  for the 3 decay modes of  $D^\pm$ . The cuts are: a)  $z > 0.4$ ;  $1.81 \leq M_{K\pi} \leq 1.92$ ; b)  $z > 0.6$ ;  $1.81 \leq M_{K\pi} \leq 1.92$ ; c)  $z > 0.4$ ;  $1.55 \leq M_{K\pi} \leq 1.70$ ;  $\cos\theta^* < 0.8$  (all masses in GeV).

The data were fitted to the total electroweak cross-section (4) with free parameters  $\sin^2 \theta_W$  and  $\alpha_s$  using parametrization II of  $\chi$ . The energy dependence of  $\alpha_s$  was taken into account and the overall normalization was allowed to vary for each experiment. The results are:

$$\sin^2 \theta_W = 0.25_{-0.03}^{+0.04}$$

$$\alpha_s(\sqrt{s} = 30 \text{ GeV}) = 0.16_{-0.04}^{+0.07}$$

This fit result is represented by the full curve in fig. 10. The best normalization factors found in this fit are indicated by the separate points on the right which have as error bars the total normalization error. The contributions from the quark-parton-model (horizontal line at  $R_{\text{had}} = 3.67$ ), the electroweak part (right hatched area) and the QCD contribution (left hatched area) are also indicated separately in fig. 10. The electroweak contribution shows a marked rise beyond cm energies of  $\sim 30$  GeV. This rise is reflected in the data. The QCD contribution on the other hand is almost independent of energy.

The QCD modification of the total cross-section is independent of fragmentation models. Therefore  $R_{\text{had}}$  gives a model-independent determination of  $\alpha_s$  if  $\sin^2 \theta_W$  is known. Leaving  $\sin^2 \theta_W = 0.217 \pm 0.02$  fixed, we obtain:

$$\alpha_s(\sqrt{s} = 30 \text{ GeV}) = 0.20 \pm 0.04 \pm 0.01$$

where the second error is due to the error in  $\sin^2 \theta_W$ . The resulting curve is the dash-dotted one in fig. 10.

The data favour the electroweak fit which gives a  $\chi^2$  of 42 for 45 degrees of freedom. A single constant value cannot be excluded however; the weighted average (with fixed normalization) is  $\langle R \rangle = 3.96 \pm 0.02$  with a  $\chi^2$  of 68.5 for 46 degrees of freedom.

#### 4.2 Axial-Vector Coupling Constants of Heavy Quarks.

The charge asymmetry of quarks is expected to be larger than that of leptons due to their fractional



charge (equ. (2)). However, the separation of individual flavours is difficult and has only been successful for heavy quarks. Two methods have been employed:

- 1) Analysis of  $D^{*\pm}$  and  $D$  decays for the c-quark
- 2) Analysis of inclusive leptons, electrons or muons, for c and b-quarks.

Method 1 was used in the published results of JADE<sup>(47)</sup> and TASSO<sup>(48)</sup> at PETRA; new data from HRS<sup>(49)</sup> will be shown here. Method 2 was used by almost all groups working at PEP<sup>(2,51)</sup> and PETRA<sup>(9,15,50)</sup>. The PLUTO<sup>(52)</sup> collaboration has found a new variable to discriminate flavours and their results will be described briefly. At the end of this chapter all available results will be summarized and compared with theory.

#### 4.2.1 $e^+e^- \rightarrow D^{*\pm}, D^0, D^\pm$ .

The  $D^-$  or  $D^{*\pm}$  mesons are assumed to contain the primary c or  $\bar{c}$  quark. This assumption is supported by the hard fragmentation function which was found in many experiments<sup>(53)</sup>.

HRS used in their analysis of  $D^{*\pm}$  decay the well known method of cutting in the mass difference  $\delta$  of  $D^{*\pm}$  and its decay product  $D^0$ . The HRS detector is particularly suited to this analysis due to its good momentum resolution. The data from  $255 \text{ pb}^{-1}$  were analysed using the following decay modes:

$$e^+e^- \rightarrow D^{*\pm} + X \quad (5.1)$$

$$\hookrightarrow D^0 \pi^\pm \quad (5.2)$$

$$\hookrightarrow K^- \pi^+ \quad (5.3)$$

$$\hookrightarrow K^- \pi^+ \pi^+ \pi^-$$

$$\hookrightarrow K^- \pi^+ \pi^0$$

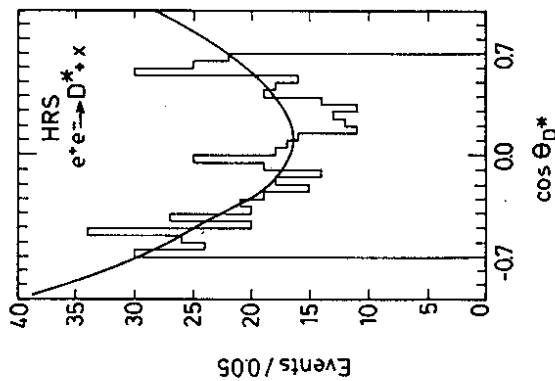


Figure 12 Angular distribution of  $D^{*\pm}$ 's; the line is a fit to the data.

No particle identification was used. In decay mode (5.3) no attempt was made to identify the  $\pi^0$ , rather the so-called  $\pi^0$  peak at 1.6 GeV in the  $K\pi$  mass distribution, which is a reflection of the decay of the  $D^0$  into  $K\pi\pi^0$ , was used. The histograms for  $\delta$  are shown in fig. 11a-c. The additional

cuts in the  $D^0$  mass and in  $z_P = 2E_P/E_{cm}$ , which were used to suppress background are listed there. For decay (5.3) an additional cut in the angle  $\theta_P^*$  of the pions in the  $D^0$  center of mass system was applied. The same cut was applied for decay (5.1) at low  $z$ -values (not shown).

The histograms show a sharp peak above a small background. For the  $K^- \pi^+ \pi^0$  decay the peak is somewhat wider due to the missing  $\pi^0$ . The angular distribution for all  $D^{*\pm}$ 's observed is shown in fig. 12 together with a fit allowing for an asymmetry. The asymmetry is  $A = -0.15 \pm 0.06$ .

HRS has also analysed the decays  $D^0 \rightarrow K^- \pi^+$  and  $D^\pm \rightarrow K^\mp \pi^\pm \pi^\mp$  by reconstructing the invariant masses. The mass peaks show up above a large background, which has to be fit simultaneously with the signal. Separate fits in the forward and backward hemisphere gave an asymmetry of  $-0.09 \pm 0.09$ .

The combined HRS result for the c-quark asymmetry is  $A = -0.14 \pm 0.05$  and the expectation from the standard model is  $-8.9\%$ , this yields an axial-vector coupling constant of  $a_c = 1.6 \pm 0.6$ .

#### 4.2.2 Inclusive Muons and Electrons.

The weak semileptonic decay of the c- and b-quark into either muons or electrons is used to separate the heavy quark from the light quarks. In addition the lepton allows the determination of the charge of the primary quark and therefore the classification into forward and backward events.

For the flavour separation all groups (except PLUTO) use the transverse momentum of the decay lepton relative to an event-axis, e.g. the thrust axis, as a distinguishing parameter. In addition most groups use an event-shape variable, which can also distinguish heavy quark from light quark decays. Almost every group has found its own "best" variable: Thrust was used by MARK J, the jet-mass and missing transverse momentum by JADE, TASSO used the sphericity of the quark jets in the jet centre of mass system and MAC has used the mass of the jet opposite to that containing the lepton.

Some groups have tried to produce an enriched event-sample by cutting in the chosen variables, others just apply weight functions in their fits. In either case Monte Carlo models have to be used heavily, either to compute efficiencies or weight functions.

PLUTO<sup>(50)</sup> has analyzed inclusive muons corresponding to  $44 \text{ pb}^{-1}$ . They have used only one variable,  $\sum_{\mu} p_T$ , the sum of the energy contained in a cone around the muon. The half opening angle of the cone was optimized at  $27^\circ$ . The distribution of data and Monte Carlo calculations are shown in fig 13a. A good separation of b-decays from the rest is observed. The angular asymmetry as a function of  $\sum_{\mu} p_T$  is shown in fig. 13b. A turn-over from negative to positive values is observed, when the b-enriched region is compared to the c-enriched region. They determine a b-asymmetry of  $-0.36 \pm 0.25$ .

In fig. 14 all axial coupling constants determined at PEP and PETRA are displayed assuming  $M_Z = 93 \text{ GeV}$ ,  $Q_c = +\frac{2}{3}$  and  $Q_b = -\frac{1}{3}$ . Although the error bars are still large, a clear difference between the coupling constants of c and b can be seen. The agreement of the experiments with each other is good. The world averages give:

$$a_c = 1.0 \pm 0.3$$

$$a_b = -0.9 \pm 0.2$$

in agreement with the prediction from the standard model of  $+1$  and  $-1$ .

## 5. SELECTED RESULTS FROM $\tau$ DECAYS

In the last months many new improved analyses of  $\tau$  decays have been presented by groups working at SPEAR, DORIS II, PEP and PETRA. The improvements are due to higher energy, more statistics and better detectors. In this chapter new results on the following topics will be presented:

- 5.1 Branching ratio  $\tau \rightarrow 5$  charged particles,  $B_5$
- 5.2 Branching ratio  $\tau \rightarrow 3$  charged particles,  $B_3$
- 5.3 Leptonic branching ratios  $B_e$  and  $B_\mu$
- 5.4 Limits on  $\nu_\tau$  mass

### 5.1 $\tau \rightarrow 5$ charged particles.

Until recently only upper limits have been published for this decay, the lowest of which was 0.16% at the 95% confidence level by the MAC Collaboration<sup>63</sup>. The experimental difficulty is -beside the low rate- recognizing the background, which comes mainly from two sources: Hadronic events and  $\tau \rightarrow 3\pi^\pm + \pi^0 + \nu_\tau$ , where one of the decay photons from the  $\pi^0$  converts in the material of the detector.

HRS<sup>61</sup>) and MARK II<sup>62</sup>) have presented the first measurements of  $B_5$ , three and two standard deviations from 0. HRS has found 10 events of the topology 1 track recoiling against 5 in a data sample corresponding to  $\sim 170 \text{ pb}^{-1}$ . The background was estimated to be 0.5 events. 5 of the 10 events have an additional  $\pi^0$  on the side of the 5 charged pions.

MARK II has analysed  $207 \text{ pb}^{-1}$ . They required that the single track is not an electron. They found 4 events with an estimated background of 0.08 events. The results for the branching ratios are:

$$B_5 = (0.13 \pm 0.04)\% \quad \text{HRS}$$

$$B_5 = (0.16 \pm 0.08 \pm 0.04)\% \quad \text{MARK II}$$

The new measurement by the JADE collaboration<sup>27</sup>),  $B_5 = (0.3 \pm 0.2 \pm 0.1)\%$  corresponding to 8 events from  $\sim 90 \text{ pb}^{-1}$ , is compatible with these values but has larger errors, which are dominated by uncertainties in the background.

### 5.2 Topological Branching Ratios.

The determination of the topological branching ratios  $B_3$  and  $B_{1 \sim 1-B_3}$  improved dramatically when data at high cm energies became available, because the separation of  $\tau$ 's from the hadronic background was easier<sup>7</sup>). The recent determinations of the topological branching ratio  $B_3$  into 3 charged particles are summarized in table 3<sup>27,29,30,63</sup>). The new world average value is  $B_3 = (13.3 \pm 0.3)\%$ .

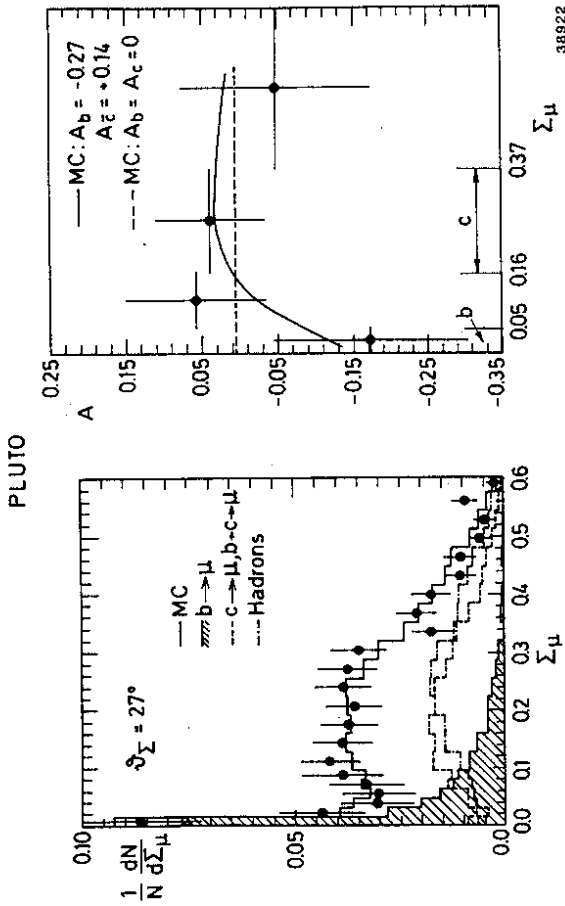


Figure 13 PLUTO analysis of inclusive muons. Details are in the text.

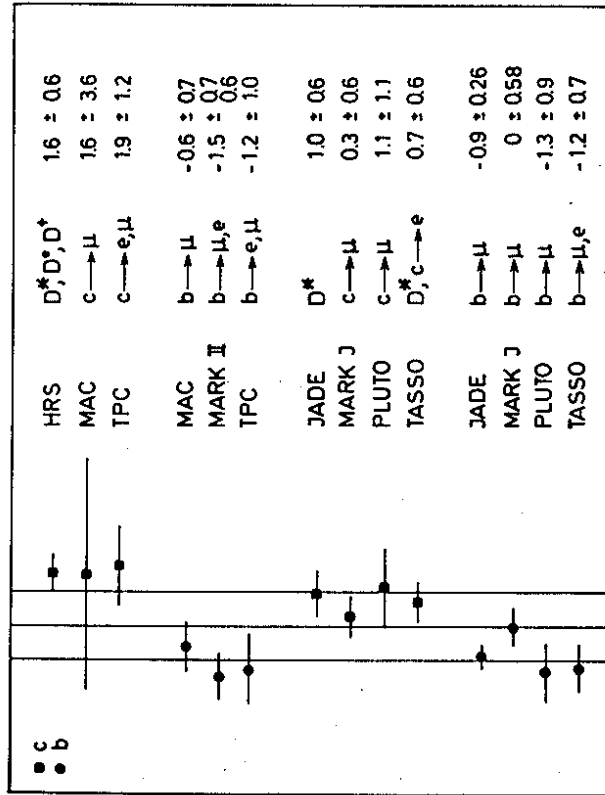


Figure 14 Axial coupling constants for c and b quarks

Table 3. Branching Ratio  $B_3$

Experiment	$B_3$ (%)
PDG 1984	$16.5 \pm 2.7$
MARK II	$14.0 \pm 2.0 \pm 1.0$
CELLO	$14.7 \pm 1.5 \pm 1.3$
TPC	$14.8 \pm 0.9 \pm 1.7$
TASSO	$15.3 \pm 1.1^{+1.3}_{-1.6}$
MAC	$13.5 \pm 0.3 \pm 0.6$
PLUTO	$12.2 \pm 1.3 \pm 3.9$
HRS	$13.0 \pm 0.2 \pm 0.3$
JADE	$13.6 \pm 0.5 \pm 0.8$
Average	$13.3 \pm 0.3$

### 5.3 Leptonic Branching Ratios.

Since the last publication of the leptonic branching ratio by the Particle Data Group, the measurements in table 4 have been made. In particular one should mention the measurement of MARK III<sup>(66)</sup> at SPEAR which was done on the  $\psi''$ . The decay leptons only have energies  $E_{\nu} \lesssim 1.5$  GeV. Therefore particle identification is easier than at PEP or PETRA, hence the small error bars.

Table 4. Leptonic Branching Ratios in %

$\tau \rightarrow e\nu\nu$	$\tau \rightarrow \mu\nu\nu$	Experiment	Reference
$16.5 \pm 0.9$	$17.5 \pm 1.5$	PDG 1984	7
$20.4 \pm 3.0^{+1.4}_{-0.9}$	$12.9 \pm 1.7^{+0.7}_{-0.5}$	TASSO 1984	30
$13.0 \pm 1.9 \pm 2.9$	$19.4 \pm 1.6 \pm 1.7$	PLUTO 1985	29
$18.2 \pm 0.7 \pm 0.5$	$18.0 \pm 1.0 \pm 0.6$	MARK III 1985	66
$17.5 \pm 0.67$	$17.1 \pm 0.77$	Average	

The weighted averages of the electronic and muonic branching ratios are also given in table 4. A constraint fit which assumes universality and which takes into account the theoretical relationship  $B_{\mu} = 0.97 \cdot B_e$  yields  $B_e = (17.6 \pm 0.5)\%$ .

The theoretical value for the decay branching ratio of the tau into electrons is given in terms of the partial decay width  $\Gamma$  and the life-time of the  $\tau$ <sup>(64)</sup>

$$B(\tau \rightarrow e\nu_e\nu_e) = \Gamma(\tau \rightarrow e\nu_e\nu_e) \cdot \tau$$

$$= \frac{G_F^2 m_{\tau}^5}{192\pi^3} \cdot \tau$$

The recent average of  $\tau$  lifetime measurements is:  $\tau_{\tau} = (2.95 \pm 0.20)10^{-13}$  sec<sup>(65)</sup>, which gives a predicted branching ratio into electrons of  $B_e = (18.5 \pm 1.25)\%$ , with which the data agree well.

### 5.4 Upper limits on the mass of the $\nu_{\tau}$ .

$\tau$  decays with a low Q-value are sensitive to the  $\nu_{\tau}$  mass. Therefore the HRS<sup>(67)</sup> and MARK II<sup>(62)</sup> group have used their five-prong  $\tau$  decays to obtain upper limits on the mass of the  $\nu_{\tau}$ . They compared the mass of the hadronic system to the theoretical prediction and obtained limits of  $\sim 120$  MeV; all upper limits in this section are at the 95% confidence level.

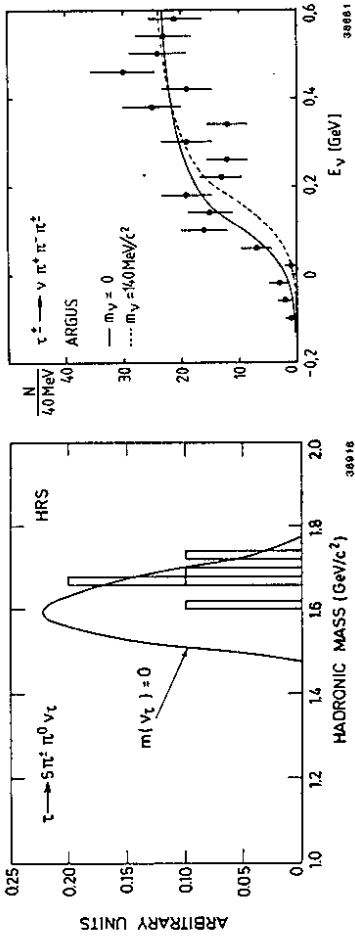


Figure 15 HRS: Mass spectrum of the 6 pions in  $\tau \rightarrow 5\pi^+\pi^0\nu_{\tau}$

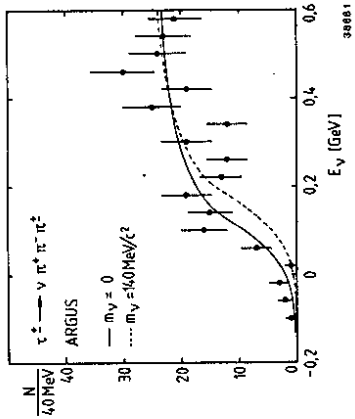


Figure 16 ARGUS:  $E_{\nu} = E_{\tau} - \sum E_{\pi}$

HRS also used the 5 events, which have an additional  $\pi^0$ . The theoretical calculation which uses CVC and the measured cross-section  $e^+e^- \rightarrow 6\pi$  is indicated in fig. 15 for  $m(\nu_{\tau})=0$ . An upper mass limit of 84 MeV was obtained.

ARGUS<sup>(68)</sup> at DORIS II has used the decay of the  $\tau$  into 3 charged particles to determine an upper limit on the  $\nu_{\tau}$  mass. They selected more than 1500  $\tau$  decays of the topology 1-3 at a  $\sqrt{s}$  of  $\sim 10$  GeV. The high end of the energy spectrum of the 3 charged pions is sensitive to the mass of the  $\nu_{\tau}$  (fig.16), whereas background would mostly contribute to low energies. Their simulation of the decay uses isotropic decays in the  $\tau$  rest frame. The prediction for the neutrino energy spectrum is shown for two values of the  $\nu_{\tau}$  mass together with the data in fig. 16. ARGUS obtains an upper limit of 70 MeV at 95% confidence level. All upper limits are summarized in table 5.

Table 5. Upper limits at 95% confidence level on the mass of the  $\nu_{\tau}$ .

Experiment	Reference	Decay	Limit $m_{\nu_{\tau}}$ (MeV)
DELCO	69	$\tau \rightarrow K K \pi \nu_{\tau}$	157
MARK II	70	$\tau \rightarrow 4\pi \nu_{\tau}$	143
MARK II	62	$\tau \rightarrow 5\pi \nu_{\tau}$	125
ARGUS	68	$\tau \rightarrow 3\pi \nu_{\tau}$	70
HRS	67	$\tau \rightarrow 5\pi \nu_{\tau}$	131
HRS		$\tau \rightarrow 5\pi^{\pm} \pi^0 \nu_{\tau}$	84
HRS		combined	82

### Acknowledgements.

I want to thank the organisers of the Trieste workshop and the Autun conference for giving me the opportunity to give this review. Thanks to all physicists from the various experiments who have helped me by providing their data. Finally I wish to thank my colleagues at DESY who have helped reading the manuscript.

REFERENCES.

- The following conferences and proceedings will be mentioned:  
 Cornell 1983 : Proceedings of the 1983 International Symposium on Lepton and Photon Interactions at High Energies, Editors D.G. Cassel and D.L. Kreinick, Cornell University, Ithaca  
 Bari 1985: Int. Europhysics Conference on High energy Physics, Bari, Italy, July 1985  
 Kyoto 1985: 1985 International Symposium on Lepton and Photon Interactions at High Energies, Kyoto, Japan, August 1985
1. S.L. Glashow, Nucl. Phys. 22 (1961), 579; Rev. Mod. Phys. 52 (1980), 539;  
 A. Salam, Phys. Rev. 127 (1962), 331; Rev. Mod. Phys. 52 (1980), 525;  
 S. Weinberg, Phys. Rev. Lett. 19 (1967), 1264; Rev. Mod. Phys. 52 (1980), 515.
  - \*2. R. Budny, Phys. Lett. 55B (1975), 227; Phys. Lett. 55B (1975), 227.
  3. W. Wetzel, Nucl. Phys. B227 (1983), 1; Preprint Heidelberg (1983); At s=1195 GeV<sup>2</sup>  
 $\Delta A = \pm 0.6\%$  and at s= 1853 GeV<sup>2</sup>  $\Delta A = \pm 1.1\%$  were used
  4. M. Böhm and W. Holfik, Nucl. Phys. B204 (1982), p. 45; Phys. Lett. 139B (1984), p. 213;  
 M. Böhm et al., Z. Phys. C 27 (1985), p. 523.
  5. F.A. Berends, R. Kleiss and S. Jadach, Nucl. Phys. B202 (1982), 63.
  6. R.W. Brown, K. Decker, E.A. Paschos, Phys. Rev. Lett. 52 (1984), 1192.
  7. Particle Data Book, Rev. Mod. Phys. 52 (1980).
  8. R.J. Cashmore et al., Oxford preprint (1985 45/85); The Forward Backward Asymmetry in  $e^+e^- \rightarrow \mu^+\mu^-$ . Comparisons between the theoretical calculations at the one-loop level in the standard model and with the experimental measurements, submitted to Z. Phys..
  9. Previous summaries are: B. Naroska, CORNELL 1983, p. 96;  
 U. Martyj, DESY preprint 84-48 (1984); Proc. 121st AIP Conf. "High Energy  $e^+e^-$  Interactions" (1984), 215, R.S. Panvini and G.B. Wood, Vanderbilt University;  
 D. H. Saxon, Physics in Collisions IV, Ed. A. Seiden, UC Santa Cruz;  
 R. Marshall, Rutherford preprint RAL 84-088 (1984). Talk at 6th General Conf. of EPS, Prague, Czechoslovakia, August 1984
  10. CELLO Collaboration, H.J. Behrend et al., Z. Phys. C 14 (1983), p. 283.
  11. CELLO Collaboration, Measurement of The Muon and Tau Pair Asymmetry in  $e^+e^-$  Annihilations at  $39.8 \leq \sqrt{s} \leq 46.6$  GeV; contributed paper to BARI and KYOTO.
  12. JADE Collaboration, W. Bartel et al., Phys. Lett. 108b (1982), p. 140.
  13. JADE Collaboration, B. Adeva et al., Phys. Rev. Lett. 48 (1982), p. 1701.
  14. MARK J Collaboration, B. Adeva et al., Phys. Reports 109 (1984), p. 133.
  15. MARK J Collaboration, B. Adeva et al., MIT Technical Report 144 (1985).
  16. MARK J Collaboration, Ch. Berger et al., Z. Phys. C 21 (1983), p. 53.
  17. PLUTO Collaboration, Ch. Berger et al., Z. Phys. C 27 (1985), p. 341.
  18. PLUTO Collaboration, Ch. Berger et al., Z. Phys. C 27 (1985), p. 341.
  19. TASSO Collaboration, M. Althoff et al., Phys. Lett. 110B (1982), p. 173; Z. Phys. C 22 (1984), p. 13.
  20. TASSO Collaboration, Muon pair production a centre of mass energies up to 46.78 GeV; contributed paper to BARI and KYOTO.
  21. HRS Collaboration D. Bender et al., Phys. Rev. D 30 (1984), p. 515;  
 M. Derrick et al., Phys. Rev. D 31 (1985), p. 2352.
  22. MAC Collaboration W. Ash et al., SLAC-PUB 3741 (1985).
  23. MARK II Collaboration N.E. Levi et al., Phys. Rev. Lett. 51 (1983), p. 1941.
  25. F.A. Berends et al., Nucl. Phys. 63B (1973), 381; DESY preprint 80-066 (1980); Nucl. Phys. 177B (1981), 237.
  26. CELLO Collaboration H.J. Behrend et al., Phys. Lett. 114B (1982), p. 282.
  27. JADE Collaboration W. Bartel et al., DESY preprint 85-065 (1985); subm. to Phys. Lett..
  28. MARK J Collaboration, private communication.
  29. PLUTO Collaboration, Ch. Berger et al., DESY preprint 85-017 (1985).
  30. TASSO Collaboration, M. Althoff et al., Z. Phys. C 26 (1985), p. 521.
  31. HRS Collab. K.K. Gan et al., Phys. Lett. 153B (1985), 116; K.K. Gan, Thesis.
  32. MAC Collaboration E. Fernandez et al., Phys. Rev. Lett. 54 (1985), p. 1620.
  34. MAC Collaboration E. Fernandez et al., MAC-NOTE-704.
  35. JADE Collaboration W. Bartel et al., Z. Phys. C 19 (1983), 197. and private communication
  36. TASSO Collaboration, M. Althoff et al., private communication.
  37. W. Krenz, Aachen preprint PITHA 84/42 (1984); submitted to Nucl. Phys. B.
  38. CHARM Collaboration, F. Bergsma et al., Phys. Lett. 147b (1984), p. 481;  
 L.A. Ahrens et al., Phys. Rev. Lett. 54 (1984), p. 18.
  39. A. Boehm, Measurement of  $\sin^2 \theta_W$  from the reaction  $e^+e^- \rightarrow \mu^+\mu^-$ , Aachen Preprint PITHA 84/11 (1984).
  40. D. Proievaux, Physics in Collisions V (1985) (to appear), Autun, France;  
 UA1 Collaboration, G. Arnison et al., Phys. Lett. 126B (1983), 398; Phys. Lett. 129B (1983), 273;
  - UA2 Collaboration, P. Bagnaia et al., Z. Phys. C 24 (1984), 1.
  41. A. Sirlin, W. J. Marciano, Nucl. Phys. B189 (1981), 442; W. J. Marciano, CORNELL 1983 (1983), p. 80.
  42. J. Jesak, E. Laermann and P.M. Zerwas, Phys. Lett. 98B (1981), p. 363.
  43. JADE Collaboration W. Bartel et al., Phys. Lett. 129B (1982), p. 145;  
 DESY preprint 85-57 (1985).
  44. MARK J Collaboration, private communication.
  45. TASSO Collaboration R. Brandelik et al., Phys. Lett. 113B (1982), p. 499;  
 M. Althoff et al., Phys. Lett. 138B (1984), p. 441; Z. Phys. C 22 (1984), p. 307.
  46. MAC Collaboration E. Fernandez et al., Phys. Rev. 31 (1985), p. 1537.
  47. JADE Collaboration W. Bartel et al., Phys. Lett. 146B (1983), p. 121.
  48. C. Youngman, Proc. XIX Rencontre de Moriond (1984), p. 173, Ed. J. Tran Thanh Van.
  49. HRS Collaboration M. Derrick et al., Phys. Rev. Lett. 53 (1984), p. 1971;  
 Phys. Lett. 146B (1984), p. 261; S. Abachi et al, Purdue Preprint PU-85-536 (1985).
  50. J. M. Izen, DESY preprint 84-104 (1984), (to appear in Proc. of 15th Symp. on Multiparticle Dynamics, Lund, Sweden 1984);  
 CELLO Collaboration H.J. Behrend et al., Z. Phys. C 19 (1983), p. 291;  
 JADE Collaboration W. Bartel et al., Phys. Lett. 146B (1984), p. 437;  
 TASSO Collaboration M. Althoff et al., Phys. Lett. 146B (1984), p. 443;  
 Z. Phys. C 22 (1984), p. 219.
  51. TPC Collaboration H. Aihara et al., Phys. Rev. 31 (1985), p. 2719;  
 Tokyo preprint UT-HE 84/03 (1984).
  52. PLUTO Collaboration Ch. Berger et al., private communication,  
 also C. Maxeiner DESY PLUTO-85-03 internal report (in german)
  53. S. Bethke, DESY preprint 85-67 (1985); and references therein.
  61. HRS Collaboration, I. Beltrami et al., Phys. Rev. Lett. 54 (1985), p. 1775.
  62. MARK II Collaboration, P.R. Burchat et al., Phys. Lett. 54 (1985), p. 2489.
  63. MARK II Collaboration, C.A. Blocker et al., Phys. Rev. Lett. 49 (1982), 1369;  
 CELLO Collaboration, H.J. Behrend et al., Z. Phys. C 23 (1984), 103;  
 TPC Collaboration, H. Aihara et al., Phys. Rev. D30 (1984), 2436;  
 MAC Collaboration, E. Fernandez et al., Phys. Rev. Lett. 54 (1985), 1624;  
 HRS Collaboration, M. Derrick et al., ANL-HEP-PR-85-05 (1985).
  64. F.J. Gilman and S.H. Rhee, Phys. Rev. D31 (1985), 1066.
  65. V. Lüth, Physics in Collisions V (1985) (to appear), Autun, France.
  66. MARK III Collaboration R.M. Baltrusaitis et al., SLAC-PUB 3732 (1985);  
 submitted to Phys. Rev. Lett..
  67. HRS Collaboration S. Abachi et al., Purdue preprint PU 85-535 (1985).
  68. ARGUS Collaboration H. Albrecht et al., DESY preprint 85-54 (1985).
  69. DELCO Collaboration G.B. Mills et al., Phys. Rev. Lett. 54 (1985), p. 624.
  70. MARK II Collaboration C. Matteuzzi et al., Phys. Rev. Lett. 52 (1984), p. 1869;  
 update submitted to Phys. Rev. D Brief Reports.